# KINEMATIC SURVEY OF HALO STARS FROM SDSS-DR2 $\cap$ GSC2

**P. Re Fiorentin**[1], **A. Spagna**[2], **A. Helmi**[3], **M.G. Lattanzi**[4]

[1]Dipartimento di Fisica Generale, 10125 Torino, Via Pietro Giuria 1, Italy
[2,4]INAF, Osservatorio Astronomico di Torino, 10025 Pino Torinese, Via Osservatorio 20, Italy
[3]Kapteyn Institute, 9700 AV Groningen, P.O. BOX 800, The Netherlands

## ABSTRACT

We present a new sample of blue subdwarfs within a few kpc of the Sun assembled from the cross-matching of SDSS-DR2 and GSC2. By means of the astrometric, photometric and spectroscopic data, we estimate distances and velocities that we use to investigate the kinematics in the inner halo and search for substructures, possible fossil signatures of past merging events.

Key words: Astrometry; Surveys; Galaxy: halo, kinematics; Gaia.

## 1. INTRODUCTION

Observations of metal-poor stars have many times been used to discriminate between alternative galaxy formation and evolution scenarios (e.g., Eggen et al. 1962; Searle & Zinn 1978).

In a CDM Universe, the first objects to form are small systems which then merge and give rise to the larger scale structures we observe today. This theory predicts the presence of substructures due to mergers and accretion that galaxies may have experienced over their lifetime. Direct comparisons to observations have shown that this model fits in reproducing both the local and the distant Universe.

Several examples of mergers and galaxy interactions have been observed in the Milky Way, such as the disrupted Sagittarius and Canis Major dwarf galaxies (e.g., Ibata et al. 1995; Martin et al. 2004), the phase-space stream of halo stars in the solar neighbourhood (Helmi et al. 1999), the tidal tails from halo globular clusters and dwarf spheroidal galaxies.

Until now, studies of the kinematics of various stellar populations in the Galaxy have long been limited – especially for the inner halo – by the availability of large samples of stars with known distances, metallicity and kinematics.

## 2. THE DATA

This study is based on *spectro-photometric data* derived from the Sloan Digital Sky Survey Data Release 2 (SDSS-DR2) and on *proper motions* derived from plate material used for the construction of the Second Guide Star Catalogue (GSC2).

The SDSS-DR2 provides 3324 deg$^2$ of imaging data, position (0.1$''$ accuracy) and $u, g, r, i, z$ multi-colour photometry (few per cent accuracy) of $\sim$ 100 million classified objects ($\sim$50 million stars) down to $r$ <20.5 (Abazajian et al. 2004). Moreover, the SDSS spectroscopic survey (2627 deg$^2$) provides spectra for approximately 35 000 selected stars of all common spectral types and radial velocities, stored as redshifts, with accuracy of roughly 5 km s$^{-1}$ for stars brighter than about $r$ $\sim$18.

The GSC2 is an all-sky data base (McLean et al. 2000), from which the GSC-2.2 has been exported, compiled from Schmidt plate surveys (AAO, POSS-I and POSS-II). It contains $\sim$1 billion objects down to $B_J$ < 22.5, $R_F$ < 20.5 and $I_N$ < 19.5 with multi-colour photographic photometry (0.10–0.20 mag accuracy) and multi-epoch positions (0.2$''$–0.3$''$ absolute and 0.1$''$ relative accuracy) that we use for proper motion evaluation.

Here we focus on the equatorial stripe (see Figure 1) which covers roughly 400 deg$^2$ within 169$^\circ$.46 < $\alpha$ <231$^\circ$.78 and $-3^\circ$.67< $\delta$ <6$^\circ$.23, corresponding to intermediate galactic latitude 42$^\circ$.34< $b$ <69$^\circ$.04. We select 3590 stars among the 17 110, from the SDSS-DR2 online query, observed spectroscopically ($v_r$) and with $r$ <19, $g$ <19. In the selected region, we identify 18 GSC2 fields with good overlap to SDSS-DR2, and compute accurate proper motions adopting the procedure described in Spagna et al. (1996). Absolute proper motions with a precision of $\sim$ 2–3 mas yr$^{-1}$ and zero point accuracy less than 1 mas yr$^{-1}$ have been derived combining plates POSS-II and POSS-I which span a large epoch difference ($\sim$ 45 yr). Such accuracy has been confirmed by external comparison with UCAC (Zacharias et al. 2004); see also discussion by Kinman et al. (2004).

After cross-matching between SDSS-DR2 and GSC2, we find 2160 stars with complete astrometric and spectro-photometric data: they have been successfully matched with an algorithm pairing on position, with each object paired to its neighbour out to a maximum radius of 1 arcsec.

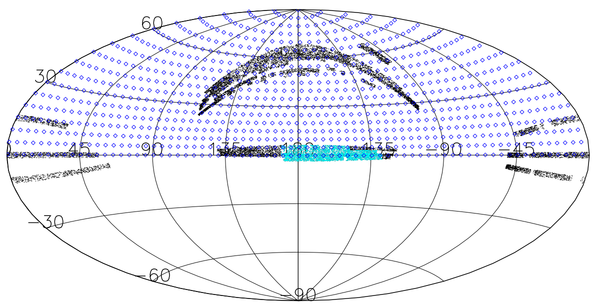


*Figure 1.* *Distribution on the sky of 17 110 stars with imaging* and *spectra data from SDSS-DR2 (dark dots). Diamonds indicate POSS-II plate centres from GSC2 in the northern Galactic hemisphere. Along the equatorial stripe, the selected region (roughly within 169° < $\alpha$ <232° and −3° < $\delta$ <7°) covers ∼400 deg$^2$. It contains 3590 stars down to $r$ <19 and $g$ <19 (light-colour dots).*

## 3. THE HALO SUBDWARF SAMPLE

For each star, interstellar extinction has been corrected using the high-resolution COBE/DIRBE dust map of Schlegel et al. (1998) extended to the SDSS photometric system (Girardi et al. 2004).

Of the 2160 stars present, we identify 290 BHB and 331 RR Lyrae by means of their characteristic colour (Sirko et al. 2004; Ivezic et al. 2000) and 129 halo metal-poor giants following the photometric classification by Helmi et al. (2003).

We choose here to focus on halo subdwarfs for which GSC2 proper motions with good S/N are available. Hence, we select those with $g - r$ >0.3 mag (cfr. halo turnoff: $g - r$ ∼0.2 mag).

Moreover, in order to check photometric classification and select such tracers, we use the Reduced Proper Motion (RPM) defined as follows (Luyten 1922):

$$H_m = m + 5\log\mu + 5 = M + 5\log V_T - 3.379 \quad (1)$$

It is an intrinsic parameter, independent of distance, which relates absolute magnitude $M$ and tangential velocity $V_T$ of a certain population to the observed apparent magnitude $m$ and total proper motion $\mu$.

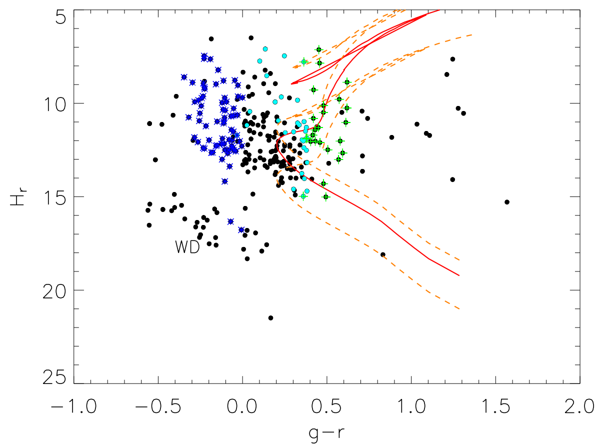


*Figure 2.* *RPM diagram based on SDSS-DR2 (spectroscopic sample) and GSC2 astrometry for stars in POSS-II field 864. Of the 297 stars with $r$ < 19 and $g$ < 19 present (dark dots), we identify 68 BHB, 32 RR Lyrae (asterisks and light-colour dots respectively) and 26 halo metal poor giants (plus signs). From Girardi et al. (2004), the $Z$ = 0.0004 isochrone with an age of 12.6 Gyr and $V_T$ = 220 km s$^{-1}$ (solid line), selection lines (dashed lines) corresponding to $V_T$ = 150 km s$^{-1}$ and $V_T$ = 500 km s$^{-1}$ overlaid.*

In Figure 2 we show the RPM diagram $H_r$ versus $g-r$ focusing on POSS-II field 864, i.e., 202°.44 < $\alpha$ <208°.84 and −3°.45< $\delta$ <2°.95. Stars photometrically classified as BHB, RR Lyrae and metal poor red giants are plotted with different symbols. The lack of red stars is due to the selection algorithm used by the SDSS to choose targets for spectroscopic follow-up.

Although the RPM diagram separates the subdwarfs from the thin disc stars and white dwarfs, there is some overlap with the locus of thick disc stars (see also analysis by Digby et al. 2003; Carollo et al. 2004).

We adopt a typical halo isochrone (Girardi et al. 2004), namely the $Z$ = 0.0004 (−1.7 dex) isochrone (solid line) with an age of 12.6 Gyr and, in order to minimize contamination and select reliably halo subdwarfs, we impose a tangential velocity range 150 km s$^{-1}$ < $V_T$ <500 km s$^{-1}$ which corresponds to the selection lines $H_{\rm min}$, $H_{\rm max}$ drawn as dashed lines in Figure 2. Notice that this criterion removes most of the thick disc stars (e.g., all objects with $V_T$ < 240 km s$^{-1}$ for $Z$ = 0.004).

## 4. KINEMATICAL PROPERTIES

After these cuts, the sample includes 118 halo subdwarf candidates with available radial velocity and proper motion. Their photometric distances, necessary for computation of full 3D kinematics, have been estimated adopting a colour-absolute magnitude relation $M_g$ versus $g-r$ (Girardi et al. 2004) assumed a mean halo metallicity $[\rm M/H]$ = − 1.3 dex with an age of 12.6 Gyr. An un-

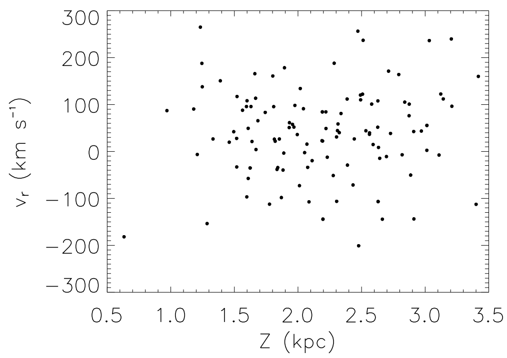


*Figure 3. Radial velocity vs. height from the plane for the* 118 *halo subdwarf candidates, within 4 kpc of the Sun. The sample covers the region 263°.39< $l$ <357°.69 and 46°.96< $b$ <68°.80.*

certainty on [M/H] of 0.5 dex, which here corresponds to about 0.35 mag in absolute magnitude, allows distances to be derived to an accuracy of roughly 20%.

This sample is distributed in the region 263°.39 < $l$ <357°.69 and 46°.96< $b$ <68°.80. For these objects, with 16< $g$ <18, we estimate a mean absolute magnitude $M_g \sim 6$ mag from which we derive distances $D$ up to 4 kpc from the Sun, corresponding to $Z_{\max}$ ~3.5 kpc. Thus, we are looking at the inner halo. In Figure 3 we show $v_r$ versus height $Z$.

Finally, we derive Galactic space velocity components $(U, V, W)$ from the given radial velocity, the measured proper motion and the distances estimated above, as follows

$$\begin{pmatrix} U \\ V \\ W \end{pmatrix} = \mathbf{G} \begin{pmatrix} 4.74 D\mu_{\alpha^*} \\ 4.74 D\mu_{\delta} \\ v_r \end{pmatrix} + \begin{pmatrix} U_\odot \\ V_\odot \\ W_\odot \end{pmatrix} \quad (2)$$

adopting the trasformation matrix $G$ from the Hipparcos data catalogue and the solar motion $(U_\odot, V_\odot, W_\odot)$ from Dehnen & Binney (1998).

## 5. RESULTS

In total, we selected 118 blue subdwarfs, within 4 kpc of the Sun, with available full 3D kinematics. The $U, V, W$ velocity distribution, shown in Figure 4(a-c), is clearly affected by the applied kinematic cuts we discussed in Section 3 (see also Figure 4(d) where the minimum threshold imposed is displayed on the $(V_\alpha, V_\delta)$ tangential velocity plane). In fact, the distribution is not gaussian and smooth as expected for a complete sample but shows some trends, regarding $W$ versus $U$ mostly.

In order to understand how different velocity cuts influence the velocity distribution, we generate 100 samples of simulated velocities according to a multivariate gaussian

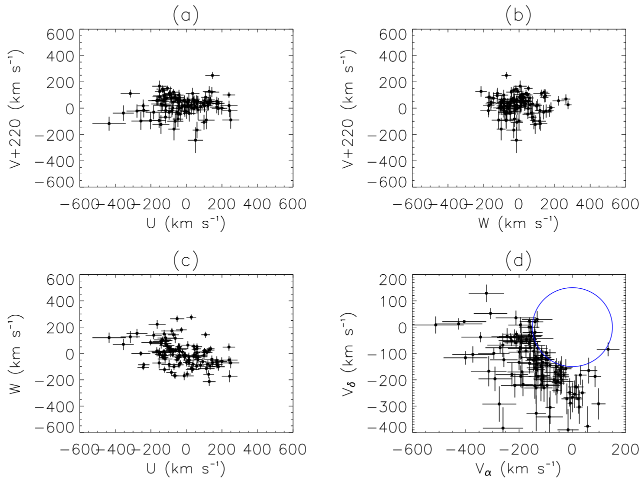


*Figure 4. Distribution of the 118 blue subdwarfs in the inner halo, selected from the 18 GSC2 fields analyzed. (a-c) Velocity projections in the $UVW$ space; (d) Tangential velocity. The circle shows the minimum velocity threshold ($V_T$ = 150 km s$^{-1}$) of the kinematically selected sample.*

halo distribution: $(\sigma_U, \sigma_V, \sigma_W)$ =(141,106,94) km s$^{-1}$ as given by Chiba & Beers (2000), and including the *same* kinematic selection criteria. As expected, all simulated velocity distributions show trends very similar to the observed one.

In Figure 5 we show the histogram of the velocity projections for our original sample (solid line) and for the simulation, an average over all realizations (dashed line). The agreement between the observed and simulated distributions is reasonably good, even though some differences are noticeable.

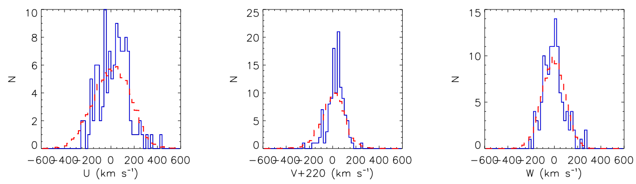


*Figure 5. Comparison of observed velocity projections with Monte Carlo simulations. Shown are histograms of $U, V, W$: for the observed 118 halo stars selected after the kinematic cut-off (solid line); for a simulated halo sample, average over 100 realizations, including the same kinematic selection criteria (dashed line).*

Can we say, to a certain level of significance, that these two data sets are drawn from the same population? How significant are the differences that we see?

We try to answer these questions by means of the Chi-Square ($\chi^2$) statistic which compares the actual observed to the simulated frequencies (Press et al. 1992).

Assuming that observations and simulations are drawn from the *same* $U, V, W$ marginal distribution, the probabilities that $\chi^2$ is greater than the measured one are listed in Table 1. Very low values indicate that the two distributions are consistent with a low significance level, i.e., that they are significantly different.

*Table 1. Probability that the Chi-Square statistic is greater than the observed one.*

| | $P(\chi^2 > \text{observed})$ |
|---|---|
| $U$ | 0.63 |
| $V$ | 0.03 |
| $W$ | 0.30 |

While $U$ and $W$ data are rather consistent with gaussian simulations under similar selection criteria, this is not the case with $V$. The observed $V$ velocity distribution is only consistent at the $3\%$ level with being drawn from a gaussian distribution after application of our kinematic selection criteria.

This result may be related to the prominent central peak present in the middle panel of Figure 5, at $-220$ km s$^{-1}$ $< V <$ $-170$ km s$^{-1}$. The feature is difficult to explain with the presence of misclassified giants; anyway, we can not exclude a residual contamination – that we are going to inquire – from high velocity thick disc stars. However if real, such an excess of stars with similar $V$ velocity could indicate further clues for substructures in the local halo.

## 6. SUMMARY

Here, we have produced a new catalogue with $U, V, W$ velocities using spectro-photometric data from SDSS-DR2 and proper motions derived from GSC2 material. 118 blue subdwarfs in the inner halo have been kinematically selected by means of the RPM diagram; their velocity distribution is quite consistent with the standard halo velocity distribution even though some clues of substructures are present.

We are going to search for kinematic substructures as predicted by CDM simulations (Helmi et al. 2002) and supported by observations in the solar neighbourhood (Re Fiorentin et al. 2004) from the all-sky catalogue of non-kinematically selected metal-poor stars (Beers et al. 2000). In order to check these results further we need to check/improve the photometric distance estimate as a function of the uncertainty on [Fe/H], check the contamination of high velocity thick disc stars and improve the selection criteria. We also plan to include more fields to increase the number of stars.

The situation will change as Gaia will collect samples of millions of stars with very accurate positions and kinematics by providing direct trigonometric distances.

## ACKNOWLEDGMENTS

We wish to thank B. McLean who kindly provided unpublished material from the GSC2 data base; R. Morbidelli, A. Volpicelli and R. Smart for archive management and valuable technical support. The GSC2 is a joint project of the Space Telescope Science Institute and the Osservatorio Astronomico di Torino. Partial financial support to this research comes from the Italian Ministry of Research (MIUR) through the COFIN-2001 program.

## REFERENCES

Abazajian, K., Adelman-McCarthy, J.K., Agueros, M.A., et al., 2004, AJ 128, 502

Beers, T.C., Chiba, M., Yoshii, Y., et al., 2000, ApJ 119, 2866

Carollo, D., Spagna, A., Lattanzi, M.G., et al., 2004, IAU Symposium 220, 207

Chiba, M., Beers, T.C., 2000, AJ, 119, 2843

Digby, A.P., Hambly, N.C., Cooke, J.A., et al., 2003, MNRAS 344, 583

Dehnen, W., Binney, J.J., 1998, MNRAS 298, 387

Eggen, O.J., Lynden-Bell, D.A., Sandage, A.R., 1962, ApJ 136, 748

Girardi, L., Grebel, E.K., Odenkirken, M., Chiosi, C., 2004, A&A 422, 205

Helmi, A., White, S.D.M., de Zeeuw, P.T., Zhao, H.S., 1999, Nature 402, 53

Helmi, A., White, S.D.M., Springel, V., 2002, Phys. Rev. D 66, 063502

Helmi, A., Ivezic, Z., Prada, F., et al., 2003, ApJ 586, 195

Ibata, R.A., Gilmore, G., Irwin, M.J., 1995, MNRAS 277, 781

Ivezic, Z., Goldston, J., Finlator, K., et al., 2000, AJ 120, 963

Kinman, T.D., Saha, A., Pier, J.R., 2004, AJ 605, L25

Luyten, W.J., 1922, Lick Obs. Bulletin 336

Martin, N.F., Ibata, R.A., Bellazzini, M., et al., 2004, MNRAS 348, 12

McLean, B. et al. 2000, ASP Conf. Ser., 216, 145

Press, W.H., Teukolsky, S.A., Vetterling, W.T., Flannery, B.P., 1992, Numerical Recipes in Fortran, The Art of Scientific Computing. Cambridge Univ. Press, Cambridge

Re Fiorentin, P., Helmi, A., Lattanzi, M.G., Spagna, A., 2004, IAU Colloquium 195, in press

Schlegel, D.J., Finkbeiner, D.P., Davis, M., 1998, ApJ 500, 525

Searle, L., Zinn, R., 1978, ApJ 225, 357

Sirko, E., Goodman, J., Knapp, G.R., et al., 2004, AJ 127, 899

Spagna, A., Lattanzi, M.G., Lasker, B.M., et al., 1996, A&A 311, 758

Zacharias, N., Urban, S.E., Zacharias, M.I., et al., 2004, AJ 127, 3043